environmental microbiology

Environmental Microbiology (2012) doi:10.1111/j.1462-2920.2012.02724.x

Minireview

# Linking environmental processes to the *in situ* functioning of microorganisms by high-resolution secondary ion mass spectrometry (NanoSIMS) and scanning transmission X-ray microscopy (STXM)

**Sebastian Behrens,[1]* Andreas Kappler[1] and Martin Obst[2]**

[1]*Geomicrobiology/Microbial Ecology and* [2]*Environmental Analytical Microscopy, Center for Applied Geosciences, University of Tübingen, Tübingen, Germany.*

## Summary

**Environmental microbiology research increasingly focuses on the single microbial cell as the defining entity that drives environmental processes. The interactions of individual microbial cells with each other, the environment and with higher organisms shape microbial communities and control the functioning of whole ecosystems. A single-cell view of microorganisms in their natural environment requires analytical tools that measure both cell function and chemical speciation at the submicrometre scale. Here we review the technical capabilities and limitations of high-resolution secondary ion mass spectrometry (NanoSIMS) and scanning transmission (soft) X-ray microscopy (STXM) and give examples of their applications. Whereas NanoSIMS can be combined with isotope-labelling, thereby localizing the distribution of cellular activities (e.g. carbon/nitrogen fixation/turnover), STXM provides information on the location and chemical speciation of metabolites and products of redox reactions. We propose the combined use of both techniques and discuss the technical challenges of their joint application. Both techniques have the potential to enhance our understanding of cellular mechanisms and activities that contribute to microbially mediated processes, such as the biogeochemical cycling of elements, the transformation of contaminants and the precipitation of mineral phases.**

Received 8 November, 2011; revised 20 January, 2012; accepted 11 February, 2012. *For correspondence. E-mail sebastian.behrens@ifg.uni-tuebingen.de; Tel. (+49) 7071 2975496; Fax (+49) 7071 295059.

## Introduction

Why do we need high-resolution techniques for chemical imaging of environmental microorganisms? Many natural biological systems consist of a heterogeneous mix of individual microbial cells, extracellular polymers, minerals, sorbed ions, transition metals, metalloids and humic substances. Abiotic and microbial catalysis of reduction and oxidation reactions drive the biogeochemical cycles of many elements on Earth (Falkowski *et al.*, 2008). These processes form redox gradients that depend on chemical composition, reduction potentials of the relevant redox couples and microbial activities (Borch *et al.*, 2010). The manifold potential combinations of electron donors, electron acceptors and carbon sources along environmental redox gradients give rise to a vast phylogenetic and metabolic diversity of microorganisms. In order to gain insights into the functioning of these environmental microbial populations and to understand their role in biogeochemical element cycling it is important to study microbial processes in the environment at the scales on which they occur. It is a major goal in microbial ecology to correlate the spatial-temporal distribution of key functional groups of microorganisms to observed physiochemical properties and patterns of biogeochemical fluxes in the environment (Gutierrez-Zamora and Manefield, 2010). A mechanistic understanding of microbial processes at the micron and submicron scale will help to further our understanding of their contributions and effects on elemental cycling or, e.g. contaminant degradation and transformation at ecosystem scales. Understanding microscale variability of both microbial activities and chemical speciation will also help to unravel the details of microbial metabolic interactions and cooperations within complex environmental communities. Advanced analytical mass spectrometry and spectro(micro)scopy tools allow for detailed investigations at the (sub)cellular, molecular and elemental level (Boxer *et al.*, 2009; Templeton and Knowles, 2009). Although each approach already is a powerful analytical tool by itself, sometimes one technique is not sufficient to

**Table 1.** Features of NanoSIMS and STXM.

| Techniques | Advantages | Limitations |
|---|---|---|
| NanoSIMS | – High spatial resolution (> 0.1 μm)<br>– Ion imaging<br>– High useful ion yield at very high mass resolving power<br>– Analysis of natural abundance isotopes<br>– Use of isotope tracers ($^{13}C$, $^{15}N$, $^{18}O$) possible<br>– Analysis of cellular trace metals<br>– Depth profiling possible | – Lack of molecular fragment or small molecule information<br>– Limited mass range<br>– Measurements under high vacuum<br>– Multi-collection ( but only 5 to 7 detectors)<br>– Varying ionization yields complicate quantification<br>– Sample surface topography should be even |
| STXM[a] | – Elemental analysis of inorganic and organic constituents<br>– Speciation (molecular structure/redox species/mineral phases) from near-edge spectra<br>– Quantitative mapping of chemical species 15 to 40 nm resolution<br>– Fully hydrated samples<br>– Tomographic imaging | – Synchrotron and beam time necessary<br>– Wet mount between two fragile silicon nitride windows<br>– Maximum samples thickness 300 nm<br>– Maintaining full hydration can be challenging<br>– (Limited) radiation damage<br>– Absorption saturation |

**a.** Modified after Neu and colleagues (2010).

unambiguously identify and localize processes. However, the simultaneous use of complementary techniques (correlative microscopy) provides mechanistic insight into microbial processes such as nutrient uptake, redox transformations, as well as microbe–microbe, microbe–mineral and microbe–host interactions.

In this article, we will focus on two ion and X-ray beam-based imaging techniques, high-resolution secondary ion mass spectrometry (NanoSIMS) and scanning transmission X-ray microscopy (STXM). Other techniques that also provide spatially resolved information on the chemical composition of single cells [such as Raman microspectroscopy, matrix-assisted laser desorption/ionization mass spectrometry (MALDI-MS), atomic force microscopy (AFM) or (Nano) desorption electrospray ionization (DESI)] have recently been reviewed (Wagner, 2009; Lin *et al*., 2011; Watrous and Dorrestein, 2011; Webb *et al*., 2011). This article is not a comprehensive review on the current literature about NanoSIMS and STXM but a synopsis of the potential of these two high-resolution imaging techniques for process-driven research in environmental microbiology and geomicrobiology. Detailed literature reviews on NanoSIMS and STXM can be found elsewhere (Hitchcock *et al*., 2002; Bluhm *et al*., 2006; Lechene *et al*., 2006; Thieme *et al*., 2007; Boxer *et al*., 2009; Orphan and House, 2009; Wagner, 2009; Neu *et al*., 2010; Watrous and Dorrestein, 2011). For in-depth explanations on sample preparation methods and materials we refer the reader to the referenced research articles. After shortly introducing both imaging techniques we will summarize highlights of their application in three particular areas of microbiology: (i) geomicrobiology and biogeochemistry, (ii) microbial biofilms and (iii) microbe–microbe and microbe–host interactions. In the end, we will give an outlook on future technical developments and discuss capabilities and limitations that arise from the possibility of applying both techniques to the same samples.

## High-resolution secondary ion mass spectrometry

The advantage of imaging mass spectrometry (IMS) is its ability to collect chemical information from biological samples (Lechene *et al*., 2006). Although IMS was first used in the 1960s (Castaing and Slodzian, 1962) (Table 1), the combination of various ionization sources with different types of mass spectrometers in the past 5 to 10 years is now offering a broad spectrum of new techniques for the chemical analysis of microbiological samples, which will impact the future of microbiology. IMS allows 2D visualization of the distribution of elements and/or molecules within biological samples and even has the potential for molecular imaging in three dimensions (3D) (Fletcher *et al*., 2011).

Microorganisms can vary greatly in size (100 nm to 750 μm) but most cells have a size between 0.5 and 5 μm in diameter. To date, only dynamic SIMS, also called NanoSIMS, provides sufficient lateral resolution for the investigation of individual prokaryotic cells (Lechene *et al*., 2006). Other IMS techniques such as static SIMS, laser desorption/ionization (LDI) IMS, matrix-assisted laser desorption/ionization (MALDI) IMS, laser ablation-inductively coupled plasma (LA-ICP) IMS and DESI IMS do not have such a high lateral resolution (Watrous and Dorrestein, 2011). The reported resolutions for these techniques range from > 100 nm up to 100 μm. The spatial resolution of IMS is controlled by the physical diameter of the primary ion beam and is inversely correlated to the ion yield. As the sampled area becomes smaller, the amount of atoms or molecules that can be removed from the sample surface will be lower, resulting in a decreased measurable signal (Guerquin-Kern *et al*., 2005).

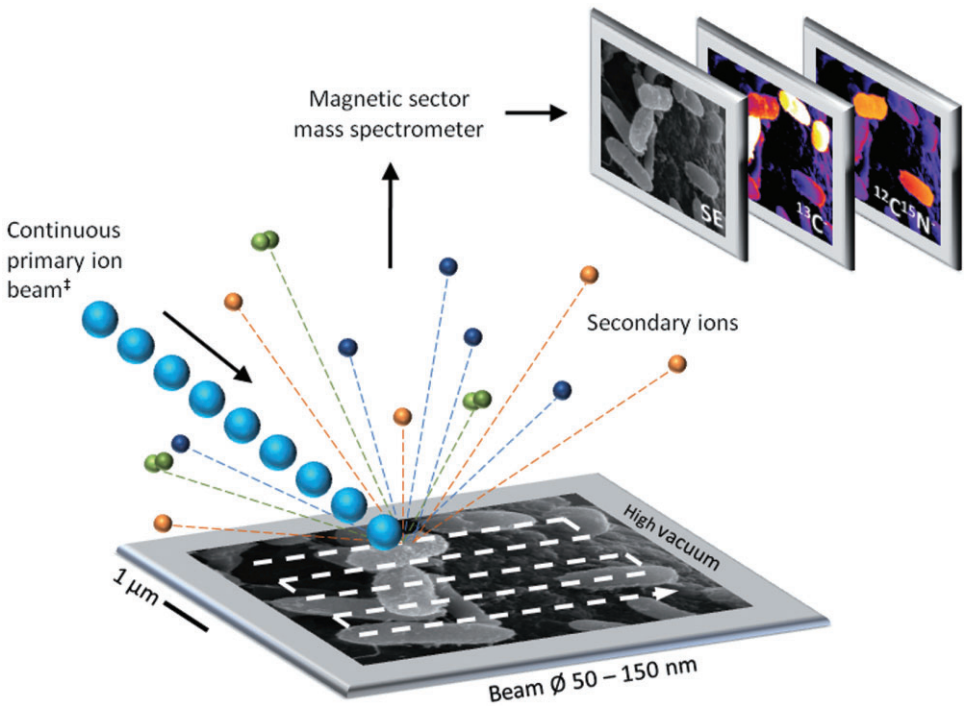


**Fig. 1.** Schematic overview of imaging mass spectrometry of microbial samples by dynamic SIMS. A beam of ions (the primary-ion beams of the Cameca NanoSIMS 50/50 L are $Cs^+$ or $O^-$) is scanned across single bacterial cells to sputter the surface atomic layers of the sample into atoms or atomic clusters. A fraction of the sputtered atoms spontaneously ionize forming so-called secondary ions. The secondary ions are characteristic of the chemical composition of the analysed sample. Ion optic technology is used to direct the secondary ions into a magnetic sector mass spectrometer where they are separated according to their mass. Because every mass can be allocated to a specific location of the sputtered sample the collected mass information can be used to create a quantitative mass image of the analysed surface. In the example shown here, images of the masses $^{13}C^-$ and $^{12}C^{15}N^-$ and the secondary ion current (SE) were generated. ‡The incident angle of the primary ion beam in the Cameca NanoSIMS 50 and 50L is normal to the sample surface, not in a 40° angle as shown. SE, secondary ions; APE, atom per cent enrichment. Modified after Watrous and Dorrestein (2011).

In Nano(dynamic) SIMS instruments the surface of a sample is bombarded with a continuous ion beam. Figure 1 illustrates the physical concept of secondary ion mass spectrometry. A primary ion beam is scanned across a couple of single bacterial cells dried onto a silicium wafer (Fig. 1). The impact of the beam triggers a cascade of atomic collisions resulting in the sputtering of a few atomic layers from the surface of the sample. Atoms and atomic clusters are ejected from the sample surface. During the ejection process, some atoms and clusters are spontaneously ionized. These secondary ions are characteristic of the chemical composition of the analysed area. The secondary ions are collected, and the secondary ion beam is directed into a magnetic sector mass analyser. An image containing quantitative information on the distribution of the selected mass in the analysed area is generated based on the quantity of secondary ion counts of the respective mass at each sputtered sample location (Fig. 1) (Guerquin-Kern *et al.*, 2005). In the newest NanoSIMS instruments up to seven mass species can simultaneously be recorded originating from the same sputtered volume. Unlike with time-of-flight (ToF-)SIMS, only preselected masses of ions are detected, and undesired ions are not measured (Boxer *et al.*, 2009).

Most commonly, an oxygen ($O^-$) primary ion beam is used to generate positive secondary ions, and a cesium ($Cs^+$) primary ion beam is used to generate negative secondary ions. The positive ionization mode can be used to image metals in biological samples, e.g. for tracking cofactors of key enzyme of metabolic processes or minerals (Mo, Zn, Ca, Fe, Al). Negative secondary ions form during the sputtering of organic biomolecules or metalloids such as arsenic ($^{75}As^-$). Important negative secondary ions are $^{12}C$, $^{13}C$, $^{16}O$, $^{18}O$, $^{19}F$, $^{28}Si$, $^{31}P$, $^{32}S$, $^{12}C^{14}N$, $^{13}C^{14}N$, $^{12}C^{15}N$ and $^{13}C^{15}N$. The sensitivity of detection of a secondary ion is dependent on the ionization probability of the respective element. For the chemical species $O^-$, $F^-$, $S^-$ and $CN^-$, the ionization probability is very high and up to 1 in 20 atoms in the sample are detected (Boxer *et al.*, 2009; Frache *et al.*, 2011). In order to image cell-(iron- or clay-)mineral aggregates, organic material and the oxides of e.g. Fe and Al need to be measured simultaneously in the same ionization mode. This can only be achieved by

analysing Fe and Al as negatively charged polyatomic species together with oxygen ($^{56}Fe^{16}O^-$ and $^{27}Al^{16}O^-$) (Heister *et al*., 2011). When oxygen is simultaneously detected its contribution can be eliminated. Clay minerals for example, can be identified by their simultaneous high signals of the negative secondary ions $^{28}Si^-$ and $^{27}Al^{16}O^-$ (Heister *et al*., 2011).

One drawback of current NanoSIMS instruments is the limited number of mass species (five to seven) that can be simultaneously detected. This often hampers the analysis of complex biological samples (Table 1), particularly samples with microorganisms, natural organic matter, minerals and various isotope ratios. In order to selectively discriminate whole cells, cell structures or molecules of interest, isotopic and/or elemental labelling has become commonplace (Behrens *et al*., 2008; Li *et al*., 2008; Musat *et al*., 2011). However, the number of elemental and/or isotopic labels that can simultaneously be applied is also often limited by the number of available detectors and the mass range of the selected secondary ions.

Another great challenge of SIMS is quantification of the elemental/isotopic sample composition. This is due to a lack of well-characterized standard materials for many of the analytes. To circumvent this problem, a species of interest can either be normalized to an element of known concentration in the sample as determined by an independent quantitative method or in the case of isotopes, mass ratios are determined (Boxer *et al*., 2009). If standards of known elemental composition are used in order to normalize species concentration within an unknown sample, it has to be taken into account that the differences in ion yield between standard and sample can be significant.

NanoSIMS is especially useful for the compositional element and isotope analysis of small samples, but because it is performed under high vacuum ($10^{-4}$ pascal or $10^{-6}$ mbar), sample preparation is crucial to maintain the morphological integrity of biological structures and cellular associations. This is usually achieved by removing water and salts while rapidly freezing the sample (Guerquin-Kern *et al*., 2005). Alternative sample preparation techniques such as air-drying and chemical fixation have also been applied but they significantly alter the structure and chemical composition of the sample (Grovenor *et al*., 2006).

### Scanning transmission X-ray microscopy

Scanning transmission (soft) X-ray microscopy combines the advantages of the chemical speciation potential of near-edge X-ray absorption fine structure (NEXAFS) spectroscopy with the possibility of quantitative analysis at a spatial resolution of 10–40 nm (depending on the focusing optics used) (Table 1). Therefore, STXM provides spatially resolved quantitative information on the distribution of elements, major biomolecules (such as proteins, polysaccharides, lipids), redox states [e.g. Fe(II) and Fe(III)] and different mineral phases with identical chemical composition.

Synchrotron-based STXM using a Fresnel zoneplate as a focusing optic was first implemented at the National Synchrotron Light Source (NSLS, Brookhaven, USA) in the 1980s (Kirz and Rarback, 1985). The technique has been further improved in the following decades, resulting in modern, interferometer-controlled microscopes that allow for an efficient acquisition of spectromicroscopic datasets (Kilcoyne *et al*., 2003).

Although the driving force for STXM development has been material sciences, in particular polymer science (Warwick *et al*., 1998), the high spatial resolution analytical capabilities of this approach have become vital to the work of biologists, geoscientists and environmental scientists (Kirz *et al*., 1995; Bluhm *et al*., 2006). Modern STXM beamlines use X-rays produced by bending magnets or an undulator. This results in delivery of soft X-rays within the energy range of 100–2200 eV (Kilcoyne *et al*., 2003; Bluhm *et al*., 2006; Kaznatcheev *et al*., 2007). This energy range is of particular interest for (geomicro-)biologists since it contains the K absorption-edges of elements of major biological interest such as carbon, nitrogen, oxygen and phosphorous, as well as the L-edges of transition metals that are highly relevant in the environment: chromium, manganese, iron, cobalt, nickel, copper and zinc. The basic principle of an undulator-based STXM beamline in standard configuration is illustrated in Fig. 2A. Soft X-rays are delivered through an undulator source, which allows for tuning both the energy and the polarization of the incoming X-rays. The energy of the X-ray beam is then selected by a monochromator with a typical energy resolving power $E/\Delta E > 3000$ which is equivalent to 0.1 eV at the C-1s absorption edge (Henke *et al*., 1993). Soft X-rays are focused by a Fresnel zone plate, and the samples are scanned through the focused light by a fast piezo-driven stage. Samples are typically mounted on polymer-film coated TEM grids, on silicon nitride windows or enclosed in wet cells made from stacked silicon nitride windows. The analysis can be performed in vacuum or under atmospheric pressure and is usually done in a He-atmosphere to avoid absorption of X-rays by $N_2$ and $CO_2$ from the ambient air. In standard configuration, X-rays are transmitted through the sample and collected using a single-photon sensitive detector. Data can be acquired as single images at specific energies, as spectra at specific positions, or as a combination of both images in sequence mode (illustrated in Fig. 2B). Thereby, images are acquired at tens to hundreds of individual X-ray energies across an absorption edge.

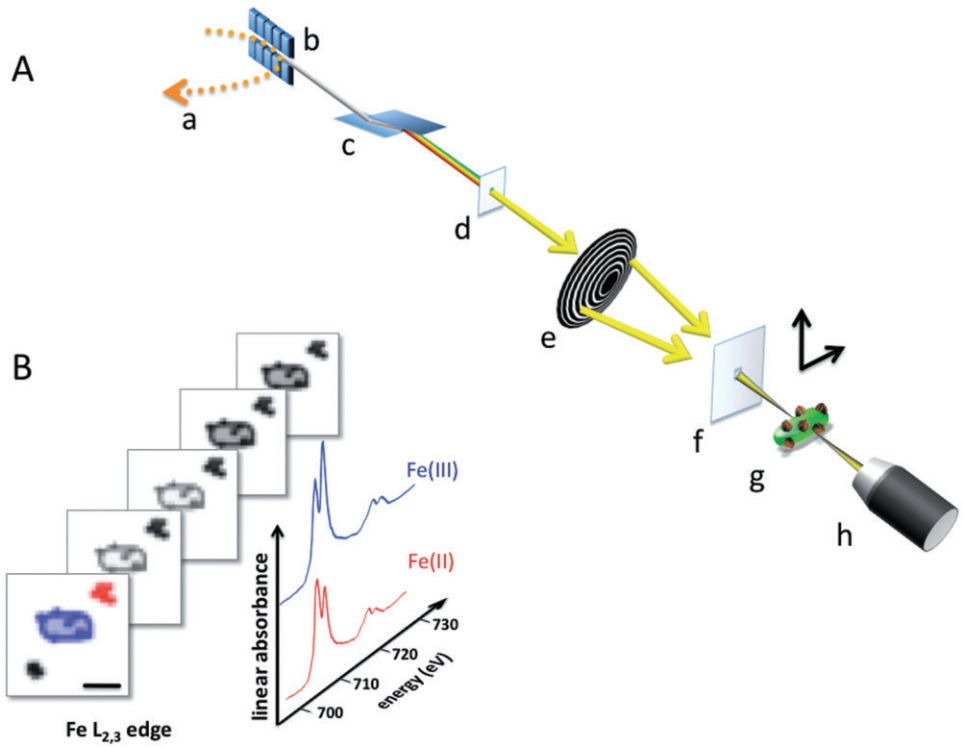


**Fig. 2.** A. Principle of synchrotron-based STXM operated in 'standard' configuration. In the storage-ring of a synchrotron (a), soft X-rays are produced by bend magnets of undulators (b). The energy of the X-rays is selected by the settings of the monochromator (c) and the position of the exit slit (d). The monochromatic X-rays are focused using a Fresnel zone plate (e). Non-focused zeroth order light is blocked by a central stop in the zone plate and a centered order-sorting aperture (f). The sample (e.g. hydrated bacteria or thin biofilms) can be scanned in both directions perpendicular to the beam axis (g). Transmitted photons are detected after conversion to visible light by a phosphorous coating using a photomultiplier tube (h).
B. Schematic of a spectromicroscopic STXM dataset acquired in image sequence mode. A sequence of tens to hundreds of images (stack) is acquired at different energies across the Fe-$L_3$ and -$L_2$ absorption edges. Each single pixel of the dataset contains the full spectral information as illustrated for an Fe(II)-oxidizing cell producing Fe(III)-enriched precipitates (blue), in contrast to an Fe(II)-dominated phase (red). From the dataset, spectra can be extracted from selected areas for the identification of chemical or redox species. Furthermore, the spectral information of each pixel can be used for pixel-based quantitative mapping of the species using either a linear decomposition approach or principle component analysis in combination with cluster analysis. Scale bar 1 μm.

Spectra from each individual pixel of the dataset can then be extracted, quantitatively analysed and be used for mapping of specific compounds.

Transmission detection combines both, one of the major advantages of STXM and one of the major limitations. The main advantage is the possibility of quantification. The transmission signal is converted into linear absorbance [optical density, $OD = -\ln (I/I_0)$, where I is the measured intensity at a specific position of the sample and $I_0$ is the reference transmitted intensity measured at an empty spot adjacent to the sample]. According to Lambert–Beer's law, OD is proportional to the amount of the respective chemical species in the beam path. The sensitivities and the detection limits strongly depend on the chemical species and the sample environment so that no general limits can be provided here. As a rule of thumb, the concentrations are in the range of a few per cent down to a few per mille (e.g. 50 mg Fe per $g_{\text{biofilm dry weight}}$) (Dynes *et al.*, 2006a; Hitchcock *et al.*, 2010).

One of the major limitations of soft X-ray STXM is sample thickness. Thick samples are not penetrated by soft X-rays due to the high photoabsorption cross-sections of light elements with K-edges at low X-ray energies (i.e. C, N, O) (Henke *et al.*, 1993) (Table 1). Typically, at the C-1s absorption edge, a sample should not be thicker than a few hundred nanometres of pure carbon. However, many (geo-)microbial samples such as cell cultures and thin biofilms fit within this range and have successfully been mapped quantitatively at the C-1s absorption edge (Benzerara *et al.*, 2004a; Dynes *et al.*, 2006a; Obst *et al.*, 2009a). The higher the energy of interest, the thicker the sample can be (up to several micrometres at the P-1s and S-1s absorption edges). The analysis of samples too thick for a specific absorption edge will result in distorted spectra. This problem can be circum-

vent by discarding potentially absorption-saturated regions of the spectra and using the remaining (minor) spectral features for quantitative mapping (Hanhan *et al*., 2009). Sample thickness can become a major limitation for hard matter samples such as mineral particles, rocks, fossils etc. One potential approach for sample preparation that has successfully been established is focused ion beam milling that is also used in preparation of thin TEM-lamella of (bio-)geochemical samples (Benzerara *et al*., 2005; Obst *et al*., 2009a).

Another advantage of STXM over similar spatially resolved analytical techniques is the possibility to analyse fully hydrated samples *in situ* such as wet biofilms (Dynes *et al*., 2006a; Hitchcock *et al*., 2009). Therefore, e.g. a droplet of a cell suspension or a hydrated biofilm is sandwiched between two 75–100 nm thin silicon nitride ($Si_3N_4$) windows, sealed using epoxy or acid-free silicone and analysed wet. This preparation avoids artefacts from drying such as shrinkage and extensive structural changes of extracellular polymers that are frequently observed in electron microscopy of air-dried or critical point dried samples (Dohnalkova *et al*., 2011). Also, wet analysis circumvents the artificial precipitation of dissolved salts that affect air-dried samples. The possibility of controlling the environment in the STXM chamber (Ghorai and Tivanski, 2010) and recent developments of a humidity-controlled measurement cell (Wang *et al*., 2011) also allow for studying the influence of humidity on water-sensitive samples under controlled conditions. Furthermore, STXM allows for analysing encapsulated samples under fully anoxic conditions (Pantke *et al*., 2012).

The contrast mechanism of synchrotron-based soft X-ray STXM is based on the excitation of core-level electrons to higher energy states such as unoccupied molecular orbitals. Therefore, the analytical capabilities of STXM are comparable to transmission electron microscopy (TEM) in combination with electron energy loss spectroscopy (EELS). In contrast to TEM–EELS, where the majority of electrons that interact with the sample do not contribute to the excitation of core-level electrons that are analysed, in STXM all photons that are absorbed by the sample contribute to the chemical information content of the resulting spectra. As a result, the beam-induced damage that is necessary in order to obtain a certain amount of chemical information was found to be significantly higher for TEM–EELS as compared with STXM (Hitchcock *et al*., 2008a). Particularly soft matter such as microbial biomass or extracellular organic components of biofilms are sensitive to radiation damage, so that STXM has a significant advantage for analytical questions over TEM–EELS, although the spatial resolution of the X-ray-based technique is an order of magnitude lower as compared with TEM.

## Examples of SIMS and STXM applications in microbiology

### *Geomicrobiology and biogeochemistry*

High-resolution chemical imaging methods such as NanoSIMS and STXM enable studies of the ecophysiology of individual microbial cells and the resulting interactions with their direct chemical environment, such as the uptake or sorption of ions, chemical species or the precipitation of mineral phases. Thus, NanoSIMS and STXM have the capacity to track the flow of nitrogen, carbon, phosphorus, sulfur, iron and other biologically active elements within microbial communities, thereby providing mechanistic insights into the role of microorganisms in the biogeochemical cycling of these elements in nature.

*Applications of SIMS in geomicrobiology and biogeochemistry.* Isotope-labelling experiments have considerably expanded our toolbox for studying the ecology and metabolic potential of microbial populations and cells in the environment (Neufeld *et al*., 2007). Most published studies incubated mixed microbial enrichment cultures or environmental samples with a heavy isotope-labelled substrate (e.g. $^{13}C$- and $^{15}N$ isotopes) and followed the incorporation of the heavy isotope into microbial biomass. In combination with SIMS, such stable isotope probing (SIP) experiments can track the distribution of isotopes and elements on a micrometre or even submicrometre scale within microbial communities, and can be used to study metabolic processes within a cell or consortium of cells.

Most recent studies have used $^{13}C$-labelled bicarbonate and $^{15}N$-labelled dinitrogen to address the contribution of carbon and nitrogen fixation by cyanobacteria or anoxygenic phototrophic bacteria from marine and freshwater habitats to ecosystem carbon and nitrogen cycling. Popa and colleagues (2007) used NanoSIMS to image the cellular distribution of the heavy isotopes of carbon and nitrogen at multiple time points during a diurnal cycle as proxies for carbon and nitrogen fixation of the filamentous multicellular cyanobacterium *Anabaena oscillarioides* (Popa *et al*., 2007). Their analysis of the temporal and spatial distribution of the newly fixed C and N revealed a tremendous heterogeneity within and between individual cells of one filament and between different filaments. This important finding was later confirmed by many other NanoSIMS studies which also observed a remarkable variability in metabolic rates of individual cells of the same species (Behrens *et al*., 2008; Musat *et al*., 2008; Finzi-Hart *et al*., 2009; Halm *et al*., 2009; Ploug *et al*., 2011).

Ploug and colleagues (2011) used NanoSIMS to study carbon and nitrogen fluxes in *Aphanizomenon* sp. colonies, a filamentous, colony-forming cyanobacterium. Together with *Anabaena* sp. and *Nodularia spumigena*,

these filamentous cyanobacteria comprise 20–30% of the cyanobacterial biomass in the Baltic Sea. Small-scale measurements of *in situ* $O_2$ fluxes using oxygen microsensors were combined with NanoSIMS analysis to determine net photosynthesis and dark respiration directly in *Aphanizomenon* sp. colonies. Based on their SIP experiments, microsensor measurements, mass spectrometry and NanoSIMS the authors concluded that *Aphanizomenon* sp. contributes significantly to the total cyanobacterial $N_2$ fixation in the Baltic Sea. A substantial fraction of the fixed N is directly released as $NH_4^+$ into the surrounding water fuelling the growth of other microbial community members in the water column and underlining the importance of *Aphanizomenon* sp. in the large-scale carbon and nitrogen biogeochemical fluxes in the Baltic Sea.

Using a similar combination of SIP and NanoSIMS Finzi-Hart and colleagues (2009) characterized metabolic uptake patterns of carbon and nitrogen of individual cells of the marine cyanobacterium *Trichodesmium*, which is ubiquitous in tropical and subtropical seas and contributes to global N and C cycling (Finzi-Hart *et al*., 2009). The unicellular *Trichodesmium* does not form heterocysts and therefore must protect its nitrogenase enzyme from the $O_2$ produced during $H_2O$ cleavage and $CO_2$ fixation. Correlated TEM and NanoSIMS were able to colocalize $^{15}N$ and $^{13}C$ hot spots temporally with cyanophycin granules. The authors speculated that besides an observed temporal segregation of $CO_2$ and $N_2$ fixation the subcellular cyanophycin storage compartment might serve to also physically separate C and N fixation thereby uncoupling both processes from growth dynamics. This study nicely demonstrates how incorporation of stable isotope labelling and modern high-resolution imaging technologies can help to unveil complex physiological mechanisms in ecologically important microorganisms.

Understanding the intricate interactions of phylogenetically and metabolically diverse microbial communities remains one of the greatest challenges in microbial ecology. Fike and colleagues (2008) used a combined NanoSIMS and fluorescence *in situ* hybridization (FISH) approach to unravel the relationships between microbial metabolic activity and the establishment of geochemical gradients in hypersaline cyanobacterial mats (Fike *et al*., 2008). In an elegant approach toward measuring microscale gradients of dissolved sulfide the authors let a small piece of silver foil react with the sulfide within the mats and analysed it afterwards for the sulfur abundance and $\delta^{34}S$ isotope composition using NanoSIMS. The 2D geochemical mapping on a scale from 1 μm to 200 μm showed distinct concentrations of sulfide in different layers of the mat with a general trend of increased sulfide concentrations at depth. Variations in sulfide concentration and isotopic composition were consistent with the spatial distribution of sulfate-reducing bacteria of the family *Desulfobacteriaceae* as determined by FISH-based cell counts. The study by Fike and colleagues (2008) is a great example of how microscale measurements of both geochemical gradients and microbial populations can provide a link between microbial activity and isotopic signatures at scales relevant for microbial processes.

Since the initial description of sulfur bacteria in the redox transition zone of Lake Cadagno, a meromictic lake in the Swiss Alps (Deldon *et al*., 1985), numerous studies on the community composition and dynamics of anoxygenic, purple and green sulfur bacteria have been published (Fischer *et al*., 1996; Schanz *et al*., 1998; Schanz and Stalder, 1998; Tonolla *et al*., 1999; 2003; 2004; 2005). More recently, Musat and colleagues (2008) and Halm and colleagues (2009) used a joined FISH-NanoSIMS approach to quantify metabolic activities of individual cells that were phylogenetically identified by FISH coupled element-labelling (Musat *et al*., 2008; Halm *et al*., 2009). They used $^{13}C$-bicarbonate, $^{15}N$-dinitrogen and $^{15}N$-ammonium to determine cellular carbon- and nitrogen-assimilation rates among different FISH-identified populations of anoxygenic phototrophic sulfur bacteria. The work gave interesting new insights into the ecological role of the different metabolic types of phototrophic sulfur bacteria. Musat and colleagues (2008) showed that *Chromatium okenii* cells, which made up only about 0.3% of the total cell numbers in the chemocline, were responsible for 40% of the total uptake of ammonium and 70% of the total carbon fixation in the system (Musat *et al*., 2008). Halm and colleagues (2009) were also able to link the genus *Chlorobium* to *in situ* nitrogen fixation in the redox transition zone and demonstrate that this taxonomic group of green sulfur bacteria is capable of at least partly compensating for an observed nitrogen loss through denitrification (Halm *et al*., 2009).

NanoSIMS has also recently been used by Tourna and colleagues (2011) to characterize carbon assimilation of the first isolate of an ammonia-oxidizing Archaeon (AOA) from soil (Tourna *et al*., 2011). Although strain EN76 (*Nitrososphaera viennensis* gen. et sp. nov.) is able to grow chemolithoautotrophically, considerably higher growth rates were only obtained after the addition of pyruvate. Based on growth experiments with $^{13}C$-pyruvate and subsequent $\delta^{13}C$-enrichment measurements of single cells by NanoSIMS, the authors quantified that less than 10% of the cellular carbon stemmed from pyruvate. This showed that carbon assimilation by the new AOA isolate was predominantly driven by bicarbonate fixation under the tested conditions. AOA are among the most abundant microorganisms on our planet but currently their role in global carbon and nitrogen cycling remains poorly understand. The study by Tourna and colleagues (2011) emphasizes the importance of obtaining and characterizing new isolates in order to constrain the

energy metabolism and carbon assimilation pathways of this environmentally relevant group of Archaea.

Byrne and colleagues (2010) used NanoSIMS to study the spatial progress of magnetite biomineralization in *Desulfovibrio magneticus* sp. RS-1 (Byrne *et al*., 2010). This specific magnetotactic bacterial strain forms bullet-shaped magnetite-crystals and iron- and phosphorous-containing granules but it was not known if the iron-phosphate granules serve as precursors of the magnetite crystals. Pulse-chase experiments with $^{57}Fe$ showed that the iron-phosphorous granules and the magnetite crystals are likely formed through separate cellular processes but dissolution of the granules does likely provide iron for magnetite crystal formation. The study nicely demonstrates how NanoSIMS can be applied to study the cellular mechanism of microbial biomineralization with subcellular resolution.

Another promising research area for IMS applications is the analysis of submicron processes in soil science. The possible applications of NanoSIMS for biogeochemical processes in soil were first reviewed by Herrmann and colleagues (2007b). They also showed for the first time that it is possible to identify bacteria after $^{15}N$ enrichment within the soil matrix. Two other recent studies describe the use of NanoSIMS for characterizing soil organo-mineral associations and soil organic matter dynamics (Heister *et al*., 2011; Mueller *et al*., 2012). The study by Heister and colleagues (2011) nicely shows how NanoSIMS can distinguish between clay and iron (hydr)oxides and how the C/N ratio can serve to differentiate between highly condensed charcoal and soil organic material. Mueller and colleagues (2012) performed soil incubation experiments with $^{13}C$ and $^{15}N$-labelled amino acids and followed the distribution of labelled organic matter in primary soil particles. The heterogeneous distribution of the isotope label within particulate organic matter clusters identified regions of increased microbial activity as well as the different sorption characteristics of intact soil organo-mineral aggregates.

*Applications of STXM in geomicrobiology and biogeochemistry.* Although the application of STXM for studying the impact of microorganisms on biogeochemical cycling is not yet as common as the use of NanoSIMS, there are a number of studies wherein STXM helped to elucidate the mechanisms that have the potential to impact global elemental cycles, in particular the carbon cycle and the cycle of redox-active transition metals such as manganese and iron. One of the major advantages of STXM is the possibility of analysing both, the inorganic and organic chemical composition, speciation and distribution of complex samples, and to identify and quantitatively map mineral phases and metabolites with moderate sensitivity.

Benzerara and colleagues (2004b) showed for the first time that the Ca-2p absorption edge can be used to unambiguously identify microbially formed Ca-mineral phases. They studied the mechanisms of mineral formation when they analysed biominerals that were formed in laboratory scale experiments by the microorganism *Caulobacter crescentus*. Under high $Ca^{2+}$ concentrations, *C. crescentus* formed calcium hydroxyapatite. Detailed understanding of the mechanisms of mineral formation is an essential prerequisite for determining the environmental conditions under which mineral phases and precipitates can be formed on regional or global scales. STXM was also applied by Obst and colleagues (2009a) to identify mineral phases and mechanisms of formation of $CaCO_3$ by the cyanobacteria *Synechococcus leopoliensis* PCC 7942. Using STXM at the C-1s and the Ca-2p absorption edges, the authors could identify a protection mechanism of the photosynthetically active cells against encrustation by $CaCO_3$, which readily precipitates when the cells take up bicarbonate ions during photosynthesis. An amorphous $CaCO_3$ layer associated with the extracellular polymers was found to have an aragonite-like short-range order and thus might prevent the thermodynamically more stable calcite from precipitating. This process does have the potential to impact the global carbon cycle since it affects the supersaturation that is necessary to overcome the nucleation barrier of $CaCO_3$ and therefore affects the precipitation of carbonates which is a major sink of atmospheric carbon.

Scanning transmission X-ray microscopy has also been proven to be an excellent tool for studying microbially mediated dissimilatory redox reactions such as the oxidation and reduction of iron. Three of the four different pathways of microbial Fe(II) oxidation, neutrophilic anaerobic phototrophic Fe(II)-oxidation, nitrate-dependent, anaerobic Fe(II)-oxidation and neutrophilic microaerophilic Fe(II)-oxidaton have already been studied with STXM. Miot and colleagues (2009a) used STXM and TEM to study the oxidation of Fe(II) to Fe(III) under anoxic conditions by the nitrate-reducing *Acidovorax* sp. strain BoFeN1. Using the difference of the Fe(II) and the Fe(III) phases in their NEXAFS spectra at the Fe-2p edges, the authors followed the successive oxidation of Fe(II) over time using STXM and found that oxidation starts in the periplasm, followed by the formation of Fe(III) minerals on the cell surface. The process finally results in a complete encrustation of the cells in Fe(III) minerals. Based on the results of Miot and colleagues (2009a), Pantke and colleagues (2012) found green rust as an intermediate phase of the Fe(III) mineral formation by the same strain. This mineral phase was found to be extremely sensitive to oxidation. However, since STXM allowed analysing samples that were encapsulated anoxically between two silicon-nitride windows, the sensitive mineral phase could successfully

be mapped around the microbial cells in the early stages of oxidation. In contrast to the nitrate-reducing strain, Fe(II) oxidation carried out by anoxigenic phototrophs such as *Rhodobacter* sp. strain SW2 does not result in cell encrustation. Miot and colleagues (2009b) found the Fe(III) minerals formed by this phototrophic strain associated with extracellular polymers. More detailed analysis of these precipitates by STXM at the C-1s absorption edge revealed the presence of lipids and polysaccharides in the organic structures associated with the minerals. Furthermore, Miot and colleagues (2009b) were able to measure a redox gradient through the Fe precipitates which appeared more oxidized in the vicinity of the cell than further away from the cell. The close association of Fe-minerals and extracellular organic compounds does suggest cellular EPS production to keep mineral precipitation away from the cell surface.

The microaerophilic oxidation of Fe(II) by bacteria at neutral pH was studied using STXM, X-ray fluorescence microscopy and transmission electron microcopy by Chan and colleagues (2009). Using environmental samples of microbial mats from an abandoned mine as well as pure cultures, the authors found Fe-minerals associated with sheath and stalk-like structures. The spectromicroscopic characterization of these structures at the C-1s absorption edge lead to the conclusion that these structures were composed of acidic polysaccharides rich in carboxylic functional groups which bind dissolved iron(III) ions and therefore control the precipitation of the Fe(III) minerals. In subsequent experiments, Chan and colleagues (2011) used STXM to prove that the stalks produced by *Gallionella ferruginea* or *Mariprofundus ferrooxydans* are rich in Fe(III) whereas no iron seemed to be bound to the cells directly. The combined microscopic approaches resulted in the suggestion of a physiological model of intracellular Fe(II) oxidation and the subsequent excretion of the oxidized iron together with the organic polymer.

Scanning transmission X-ray microscopy does not only allow for geochemical characterization of biogenic precipitates, but also for a more material science-oriented characterization of biominerals. Lam and colleagues (2010) studied the formation of magnetosomes by the magnetotactic marine *Vibrio* sp. strain MV-1 using STXM. The X-ray circular magnetic dichroism effect enabled the authors to verify that the magnetic moment of linear chains of individual magnetide crystals in magnetosomes were arranged in parallel. The spectral shape at the Fe-$L_3$ and -$L_2$ edges lead the authors to the conclusion that the magnetite of individual magnetosomes contains an excess of Fe(II) as compared with stoichiometric bulk magnetite.

In summary, Earth's elemental cycles are affected by atmospheric and biogeochemical processes but also by anthropogenic activities. One of the greatest future challenges for a better understanding of biogeochemical cycling of Earth's elements will be to distinguish human effects from natural variability. For this of course different temporal and spatial scales of relevance must be taken into account. Microorganisms act on the micro-scale while elemental cycling bridges dimensions from atomic to global. The NanoSIMS and STXM studies summarized above present great examples how chemical imaging facilitates the investigation of physiological mechanisms and environmental conditions at the $\mu m^2$ scale that each will provide a piece to the complex puzzle of a comprehensive understanding of large-scale biogeochemical processes.

### *Microbial biofilms*

Biofilms are assemblages of microorganisms and their associated extracellular products (poly-saccharides, proteins, DNA) that typically occur at environmental interfaces where microbes are mostly but not exclusively attached to a surface (abiotic or biotic) (Davey and O'Toole, 2000). Because of their heterogeneous composition, microbial biofilms provide an ideal subject for quantitative analytical imaging techniques that allow *in situ* analysis of the structure, composition, processes and dynamics of microbial communities. Again, SIMS and STXM are addressed specifically here. For a recent review of advanced imaging techniques for the assessment of biofilms composition and function including a discussion of STXM, please consult Neu and colleagues (2010).

*Applications of SIMS to biofilms.* Fayek and colleagues (2005) used the ion-imaging capabilities of NanoSIMS to characterize bioprecipitated uranium mineral phases in association with *Geobacter sulfurreducens* biofilms (Fayek *et al*., 2005). Biofilms were grown on silicon wafers in the presence of uranium-rich synthetic groundwater. Isotopically labelled $^{13}$C-acetate was used as electron donor in order to correlate biomass synthesis and radionuclide precipitation. The results of this study showed that biosequestration of uranium was enhanced by addition of acetate. Uranium precipitated as nanocrystals of uraninite ($UO_2$) on the surfaces of the *G. sulfurreducens* cells and the biofilm protected the $UO_2$ from re-oxidation. The authors concluded that *G. sulfurreducens* can immobilize uranium even under relatively oxidizing conditions with broad implications for uranium mobility and toxicity in the subsurface and potential remediation strategies.

Whereas the influence of (labelled) substrate availability was the focus of the previous example, it is also possible to derive information on the source of nutrients and electrons within biofilms for microbial growth. Using a NanoSIMS approach, Cockell and colleagues (2010)

examined the colonization and weathering of young seafloor basaltic glass from the mid-Atlantic Ridge by deep-sea microbial communities (Cockell *et al*., 2010). They detected microbial biofilms which grew in fractures and on the surface of the basalt. Biofilm formation at the fracture boundaries did not result in biogenic alteration features in the basaltic glass. The study provided evidence that the interior of young basaltic glass harbours a vital microbial community and demonstrated that the glass itself does not serve as primary source of electrons and nutrients for the developing communities.

NanoSIMS is also a powerful tool for medical microbiologists. Studies of the functioning of microbial populations colonizing various parts of the human body are still a major challenge of current medical research. By combining NanoSIMS with an isotopic tracer labelling experiment, Behrens and colleagues (2008) demonstrated that it is possible to study the fate of $^{13}$C-amino acids in complex oral biofilms while individual cells of *Cytophaga-Flavobacterium* species were identified simultaneously by halogen depositing FISH (Behrens *et al*., 2008).

*Applications of STXM to biofilms.* Lawrence and colleagues (2003) used a combination of STXM, laser scanning microscopy and TEM to map the structure and composition of river biofilms together with their extracellular polymer-matrix (Lawrence *et al*., 2003). The analytical capabilities of STXM at the C-1s absorption edge allowed for quantitative mapping of the organochemical composition of the biofilm using the intrinsic absorption contrast caused by the chemical bonds of large biomolecules.

In addition to the general organo-chemical composition that was analysed in the previous study, also the selective accumulation of organic contaminants within biofilms such as the antimicrobial chlorhexidine can be measured within an organic matrix as shown by Dynes and colleagues (2006a). When the authors exposed the river biofilms to chlorhexidine and quantitatively mapped the distribution of chlorhexidine and the major biomolecules, they found an extensive accumulation of the antimicrobial compound within lipid-rich compartments of diatoms and bacteria and could therefore identify a significant source of the compound in the food-chain.

Whereas the former study focused on mapping the distribution and accumulation of organic contaminants, Dynes and colleagues (2009) studied also the influence of the antimicrobials triclosan, benzalkonium chloride, chlorhexidine dihydrochloride and trisodium phosphate on the quantitative distribution of proteins, polysaccharides and lipids in a model biofilm of *Pseudomonas fluorescens.* Even at sub-inhibitory concentrations they found a substance-dependent change of cell morphologies and variations in the spatial distribution of the major constituents of the biofilms. However, STXM was not only applied to gain information on the organochemical composition of biofilms, but to study the interactions of biofilms with their inorganic chemical environment.

By using soft X-ray NEXAFS spectroscopy, STXM can not only be applied to investigate the distribution of organic compounds within a biofilms, but it also provides detailed insights into the distribution of inorganic components or chemical redox species. Using STXM, Dynes and colleagues (2006b) studied the distribution and association of metals with the different inorganic and organochemical components of hydrated river biofilms. Within wet samples of biofilms composed of bacteria and algae, the authors acquired spectromicroscopic data across the 2p edges of iron, manganese and nickel to quantitatively map the speciation and distribution of these metals within the biofilm. Additionally, they acquired image sequence data across the C-1s and O-1s absorption edges to also quantitatively map the organochemical composition of the biofilms and to discuss the metal distribution in the context of the biofilm composition. As a result, they showed a close association of $Ni^{2+}$ with Mn-oxides without any drying artefacts in a naturally hydrated biofilm.

Based on these results, a more detailed study of Ni-sorption in a natural river biofilm was conducted by Hitchcock and colleagues (2009). They extended the range of analysed elements to the respective absorption edges C-1s, O-1s, Ni-2p, Ca-2p, Mn-2p, Fe-2p, Mg-1s, Al-1s and Si-1s. Within the dense and heterogeneous biofilm matrix, different distinct morphologies such as sheaths of filamentous bacteria and rod-shaped cells as well as $CaCO_3$ minerals, muscovite-like minerals and $SiO_2$ could be identified. The $Ni^{2+}$ that was amended to the river water after the growth of the biofilms was found to be selectively adsorbed onto the sheaths of the filamentous bacteria, whereas the rod-shaped cells seemed to have a lower affinity to the metal ions. This detailed STXM analysis revealed that natural river biofilms play an important role in the sequestration of toxic heavy metals.

The fate of Cu nanoparticles in river biofilms was studied by Lawrence and colleagues (2011). Although the particles were only 30 nm in size, which is close to the resolution limit of STXM, their initial distribution and even their successive dissolution was followed using STXM, which allowed for identifying the redox speciation of Cu in the system. Bacteria and cyanobacteria present in the biofilms did not sorb significant amounts of the resulting dissolved Cu(II) ions, whereas Cu(II) was found to accumulate in lipid-rich EPS associated with diatoms.

In contrast to the previously mentioned examples wherein the distribution of contaminants was studied, it is also possible to probe and map chemical properties such as redox zonation within a biofilm using STXM. Hunter and colleagues (2008) studied the influence of chemical

 

microenvironments in *Pseudomonas aeruginosa* biofilms that were grown under oxic conditions with Fe(III) amended to the growth medium. The authors mapped the speciation of iron associated with the biofilms and found Fe(III) mostly enriched and associated with the cell surfaces whereas Fe(II) was localized within the polysaccharide-rich matrix of the biofilms. Since *P. aeruginosa* was found not to be able to directly reduce Fe(III), an indirect reduction mechanism was suggested to be responsible for the Fe(II) content in the biofilm.

The microbial oxidation of Mn(II) and the resulting precipitation of Mn(III) and Mn(IV) containing oxides within a microbial biofilm formed by *Pseudomonas putida* cells was studied by Toner and colleagues (2005). Using STXM, the authors for the first time identified, localized and quantified Mn(III), an environmentally highly relevant oxidant that occurred as an intermediate phase during the microbially mediated oxidation process.

Whereas SIMS can provide detailed insights into metabolic processes at the single-cell level such as the consumption of isotopic labelled substrates, STXM is useful for gaining insights, e.g. into (geo-)chemical aspects of biofilms by providing quantitative distribution of both inorganic or organic contaminants and their influence on structure and chemical composition of a biofilm. Combining both aspects by applying STXM and SIMS measurements on the same sample will allow linking information on the effect of metabolic processes on the (trans-)formation of (geo-)chemical products within a biofilm. This could for example allow for direct measurements of the influence of substrate concentrations on the decomposition and distribution of organic contaminants within biofilms, or for quantifying the consequences of changing substrate availabilities on redox zonation and thus the (im-)mobilization potential of toxic metals on the micro-scale.

### *Microbe–microbe and microbe–host interactions*

Effective identification and characterization of microbe–microbe or microbe–host interactions as they occur in the environment requires high-resolution, single-cell techniques that go beyond classical cultivation and (meta-) genomics approaches. The physiology and functioning of environmental associations between microorganisms and microbial symbionts and their host are significantly affected by spatial arrangement and the proximity of individual members. The analysis of such structures requires microanalytical techniques that preserve spatial information while facilitating the simultaneous collection of chemical and isotopic data of the associated partner cells.

*Applications of SIMS to study microbial interactions.* In order to link microbial identification to metabolic activity and substrate exchange at the single-cell level SIMS has been combined with FISH. In 2001, Orphan and colleagues were the first to use SIMS on a natural microbial consortium (Orphan *et al*., 2001). They used FISH to identify microorganisms and correlated the probe-conferred fluorescence signal to natural abundance isotope analysis with a low lateral resolution SIMS instrument (~ 1 μm beam diameter). Insights into the physiology of the methanotrophic Archaea in the consortium (ANME-2) were revealed by the large natural fractionation in carbon isotopes. The $^{13}C$-depletion of cellular biomass indicated assimilation of isotopically light methane into specific archaeal cells. In another study using the same approach the authors further provided direct evidence for the involvement of another archaeal group (ANME-1) in the anaerobic oxidation of methane at deep-sea methane seeps (Orphan *et al*., 2002).

A number of more recent publications combine stable isotope tracers ($^{13}C$- or $^{15}N$-labelled substrates) and FISH using fluorescent and halogenated oligonucleotide probes to visualize and chemically analyse specific microorganisms that have incorporated a particular substrate into their biomass. A nice example of this approach is provided by Dekas and colleagues (2009) in which SIMS imaging of deep sea Archaea revealed that they fix and share nitrogen in methane-consuming microbial consortia with sulfate-reducing bacterial symbionts (Dekas *et al*., 2009). While the archaeal/bacterial consortia have previously been described as a major sink of methane in benthic ecosystems, this study identified them as a source of bioavailable nitrogen within the ecosystem. A follow-up study by Orphan and colleagues (2009) on the same microbial consortia focused on the metabolic activity of individual consortia with special emphasis on tracking $^{15}N$-assimilation in relation to aggregate organization and size (Orphan *et al*., 2009). The study showed that metabolic activity of the methane-oxidizing Archaea was independent of aggregate size and not significantly enhanced within cells that were in direct contact with the sulfate-reducing bacteria. On the other hand, the metabolic activity of each cell type was observed to be greater in the case of the consortia compared with the methanotrophic archaea and sulfate-reducing bacteria observed alone.

Behrens and colleagues (2008) used FISH and NanoSIMS to unveil the exchange of fixed carbon and nitrogen in a co-culture of a filamentous diazotrophic cyanobacteria (*Anabaena*) and an alphaproteobacterial epibiont (*Rhizobium*) which directly attached to the heterocyst (Behrens *et al*., 2008). Epibiont cells not attached to a heterocyst of the cyanobacteria did not show $^{13}C$ or $^{15}N$ enrichment emphasizing the importance of direct cell–cell contact for C/N scavenging by the epibiont. Similarly, ion imaging by NanoSIMS was used to reveal rates of $N_2$ fixation and the transfer of nitrogen from filamentous

heterocystous cyanobacteria (*Richelia* and *Calothrix*) to their diatom partners (*Hemiaulus*, *Rhizosolenia* and *Chaetoceros*) in natural species associations (Foster *et al*., 2011). The authors nicely demonstrated that the diatom partners influence the growth and metabolism of their cyanobacterial symbionts which had 171–420 times higher $N_2$ fixation rates when the cells were symbiotic compared with the rates estimated for free-living cells. In another pioneering study NanoSIMS also provided evidence for the transfer of fixed nitrogen by bacterial symbionts living in the gill bacteriocytes of the shipworm *Lyrodus pedicellatus* (Lechene *et al*., 2007).

The rhizosphere constitutes a heterogeneous soil ecosystem in which microbes interact and compete with each other and with plant roots for nutrients. Unravelling the interplay between the heterogeneity of the physical and chemical soil composition and its impact on biological processes requires suitable methods for the reliable detection, visualization and quantification of rhizosphere processes *in situ* at the submillimetre scale. Clode and colleagues (2009) applied NanoSIMS to study the competition for nitrogen, and nutrients that exists between plants and microorganisms within the rhizosphere (Clode *et al*., 2009). Using isotope tracers they performed a spatial mapping of assimilatory processes and nutrient transfer between soil, plant and microorganisms in the rhizosphere of the wheat *Triticum aestivum*. The study is a nice example of how NanoSIMS can be used to visualize and measure soil–microbe–plant interactions. The study provided spatially resolved evidence for the assimilation of $^{15}N$ by individual microorganisms competing within the root (endorhizosphere), on the root surface (rhizoplane) and in the external soil (ectorhizosphere). NanoSIMS has also been used to study uptake, transport and subcellular distribution of arsenic and silicon in rice roots (*Oryza sativa*) (Moore *et al*., 2011). Currently, the role of rhizosphere microbial communities on the accumulation of arsenic by rice plants is largely unknown. In the near future both NanoSIMS and STXM hold great promise to make a vital contribution to better understand the intricate interplay of iron, arsenic, microorganisms and rice plant roots in a soil matrix.

*Applications of STXM to study microbial interactions.* So far studies on microbe–microbe and microbe–host interactions using STXM are scarce. Norlund and colleagues (2009) investigated microbial consortia from an acid mine drainage ecosystem and identified an active sulfur redox cycle within the microbial consortium composed of a chemoautotrophic sulfur-oxidizing *Acidithiobacillus* sp. strain and the heterotrophic sulfate reducer *Acidiphilium* sp. (Norlund *et al*., 2009). The two strains were found to syntrophically couple oxidation and reduction of sulfur thereby efficiently (re-)cycling the sulfur. STXM at the S-1s and at the S-2p edges allowed for mapping of products and intermediates in the cell aggregates and the surrounding EPS. The authors identified sulfur compounds with three different oxidation states – elemental sulfur, sulfite and sulfate – in the aggregates. The combination of STXM and visible light microscopy helped elucidating the metabolic interplay of the two microorganisms. Furthermore, the results of this study indicated that the spatial arrangement of the two strains also affected the interaction of the consortia with their environment.

It is becoming more and more evident that in nature intimate interspecies interactions prevail and constitute a fundamental component of the ecology of microbial communities. Yet microbe–microbe associations are very challenging to characterize. Advanced analytical imaging techniques, such as NanoSIMS and STXM, when combined with stable isotope or element labelling, offer the lateral and chemical resolution to study metabolic interactions between known or even uncultured microorganisms in the environment. Most recent studies focused on the partitioning of nitrogen or carbon between species but also investigations of interspecies sulfur cycling (as shown in the STXM example) hold great promise for future applications. Defining who is associated with whom, and characterizing the chemical basis of an association is prerequisite for the identification of mechanisms that affect the rates of element and nutrient exchange between species.

## Future technical developments

### *Secondary ion mass spectrometry*

NanoSIMS is a powerful tool that allows microbiologists to study the chemical composition of individual microbial cells in their natural systems in a way that has so far not been possible. However, current SIMS instruments either combine a high mass resolving power (isotope imaging) with a lateral resolution suitable for subcellular analysis of single prokaryotic cells ($< 0.1$ μm) but suffer from a low mass range (also due to the high energy primary ion beam; NanoSIMS) or they combine a lower mass resolving power with a broader mass range (suitable for the analysis of small molecules or molecular fragments) at a spatial resolution unsuitable for the analysis of subcellular features in prokaryotes (ToF-SIMS) (Watrous and Dorrestein, 2011). The combination of high lateral resolution with high mass range is challenging because the secondary ion yield decreases with the volume of the sputtered sample. In recent years the development of cluster and polyatomic ion sources (Bi, Au, $C_{60}$, Ar) made low damage surface sputtering with high ion yield possible. With state-of-the-art ToF-SIMS instruments it is now possible to record mass spectra of biological samples with a

lateral resolution below 0.2 μm (Winograd and Garrison, 2010; Fletcher *et al*., 2011). One major drawback of the current ToF-SIMS instruments is the lack of a commercially available high-resolution mass spectrometer coupled to one of the cluster primary ion sources, except for prototype instruments (Fletcher *et al*., 2008), and a lack of sensitivity in the mass range, above m/z 1000–1500 (Fletcher *et al*., 2010). In order to increase the sensitivity of detection, future technical developments should also further explore the possibilities of detecting neutral molecules by laser post ionization (Willingham *et al*., 2008; Ishihara *et al*., 2010). Another great leap forward would also be the integration of SIMS (high spatial resolution and low mass range) with MALDI-MS (soft ionization and high mass range) and electron microscopy (high spatial resolution of surface and subcellular structures). Through the pairing of mass spectrometry with electron microscopy it should be possible to identify and localize ultrafine subcellular structures and gain mass spectrometric data on their chemical composition. A prerequisite for the combination of SIMS with MALDI-MS and electron microscopy will be a sample preparation method that works for all analyses and the undisturbed transfer of samples between instruments. This requires the modification of each of the three instruments with a compatible and interchangeable cryo-stage that allows the transfer of cryo-fixated samples between the SIMS, the MALDI-MS and the electron microscope. Once samples have been cryo-prepared they can first be imaged by electron microcopy and then transferred to a MALDI-MS or SIMS instrument to record mass spectra with different spatial resolution without thawing the sample or the need for a different sample matrix. Metzner and colleagues (2008) applied cryo-SIMS and superimposed the mass spectrometric data onto high-quality cryo-SEM images of the same sample in order to study nutrient distributions in plant tissues (Metzner *et al*., 2008). At higher spatial resolution a similar approach would enable unprecedented insights into the physiology of individual microbes *in situ* and thereby the complex nature of microbial processes in the environment. Correlative image analysis strongly depends on suitable software packages. Polerecky and colleagues (2012) recently published a software program for the analysis of NanoSIMS data. Among other features the software allows manual and automated analysis of regions of interest based on information derived from NanoSIMS data and externally acquired fluorescence images, a very useful tool for environmental microbiology applications. The implementation of statistical tools also allows for the synthesis and comparative analysis of results from many different datasets. Since it is an open-source freeware program it might even be expandable to allow correlative analysis of STXM data.

### *Scanning transmission X-ray microscopy*

(Geo-)microbiological or environmental samples are usually three-dimensional (3D) assemblages of microbial cells, extracellular polymeric matrixes, minerals, sorbed ions associated with the mineral phases and organics. However, chemically sensitive imaging techniques often result in two-dimensional maps of either the surface composition of the sample, or represent 2D projections of the 3D composites. As a result, correlations between chemical species based on 2D datasets represent 'mixed' phases. This problem can partially be circumvented by analysing the samples in 3D with angle-scan tomography. Here we solely focus on 3D spectrotomography, which combines 3D spatial information with chemical specificity. Chemically non-specific soft X-ray tomography is an established technique that was shown to be useful for environmental applications for which chemical specificity is not essential (Thieme *et al*., 2003). In their first chemically specific STXM tomography experiments, Johansson and colleagues (2007) analysed aqueous suspensions of polymer microspheres at the O-1s absorption edge (Johansson *et al*., 2007). The first samples were mounted in glass microcapillaries that prevented the analysis of the C-1s edge because of the high X-ray absorption of glass in this energy region. The use of thinner carbon micropipettes instead of glass was the first successful approach to solve this problem (Hitchcock *et al*., 2008b). Obst and colleagues (2009b) used stripes of formvar-coated TEM grids as a sample support structure for STXM tomography. The authors measured the distribution and quantitative correlation of organic carbon and calcium at the C-1s and the Ca-2p absorption edges respectively, with this methodology. The major challenges of STXM tomography are a stable (i.e. low-vibration) sample mounting, the slow data acquisition due to the lack of eucentric tomography mounts, and a lack of necessary software tools for quantitative 3D correlation analysis. It can be expected that the first two limitations can be overcome with improved tomography stages or in the next generation of STXM instruments that allow for both zoneplate and sample scanning (e.g. beamline 5.3.2.1 at the ALS, which is currently commissioned). The software limitation will be overcome as more users begin to apply this powerful approach to their work.

So far STXM was limited by a relatively modest sensitivity with a detection limit in the range of 0.1% (Hitchcock *et al*., 2010) when using absorption contrast for detection. These limitations are in particular relevant for transition metals and metalloids that do not have strong resonance absorption peaks and that often appear at relatively low concentrations in the samples (e.g. arsenic). These limitations could recently be overcome by the implementation of low-energy X-ray fluorescence (LE-XRF) detection,

which lowered the detection limit for, e.g. arsenate by at least one order of magnitude (A.P. Hitchcock, pers. comm.).

Low-energy X-ray fluorescence detection was implemented by Kaulich and coworkers in the TwinMic microscope, a combined fullfield and scanning transmission X-ray microscope at the Elettra beamline in Italy (Kaulich *et al*., 2003). Fluorescence detection can be used simultaneously with transmission detection (Gianoncelli *et al*., 2009). Hitchcock and colleagues (2010) also performed preliminary experiments using fluorescence detection in addition to the transmission signal at the 11.0.2 STXM at the Advanced Light Source (ALS) in Berkeley. The implementation of LE-XRF is also planned for the STXM at beamline 10ID-1 of the Canadian Light Source (CLS) in Saskatoon.

## Outlook – combining STXM and NanoSIMS

The combination of NanoSIMS and STXM offers unprecedented opportunities for process-oriented, functional studies of environmental microorganisms. To date, the potential of each method and their potential use in tandem have not been sufficiently utilized.

Understanding how microorganisms catalyse redox reactions of Earth's elements is a major challenge of microbial ecology and geomicrobiology to date and requires mechanistic studies at the single-cell level that combine information on elemental redox speciation with uptake and incorporation of isotopic tracers in order to study dissimilatory and assimilatory metabolic activities of individual microbes. This can be achieved by the combination of chemical imaging techniques such as NanoSIMS and STXM, which can provide quantitative information on the distribution of elements, their isotopes and redox speciation at spatial resolutions relevant for microbial processes. A schematic dataset of the subsequent application of STXM and NanoSIMS on a culture of an autotrophic iron-oxidizing bacterium grown on $^{13}$C-bicarbonate is shown in Fig. 3. The figure illustrates how chemical image data of STXM and NanoSIMS could be correlated to link microbial growth (*de novo* synthesis of

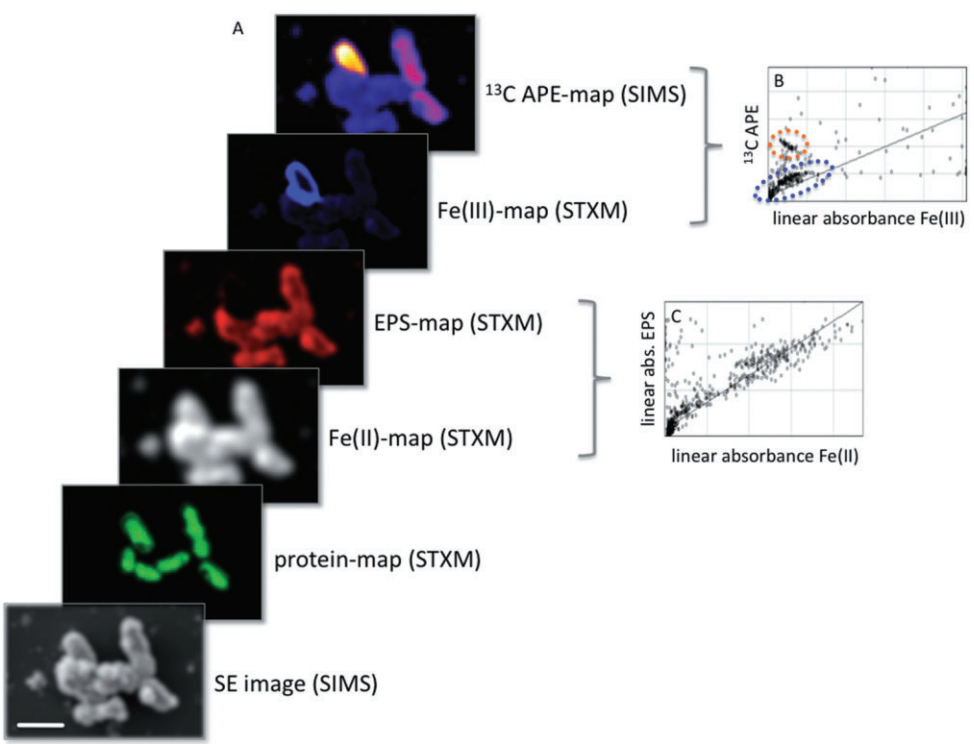


**Fig. 3.** A. Idealized schematic (no real data) of the correlative analysis of chemical species maps derived from SIMS and STXM. Atom per cent enrichment maps derived from SIMS analysis of stable isotope-labelled samples can be correlated to quantitative, linear absorbance maps of chemical or redox species derived from STXM analysis. Scale bar 1 μm.
B. The combination of SIMS and STXM allows for linking information on assimilatory (e.g. carbon fixation) and dissimilatory (e.g. iron oxidation) microbial activities, and will facilitate the analysis of metabolic mechanisms. Blue dotted circle: correlation of $^{13}$C-SIMS and Fe(III)-STXM data, indicative of iron-oxidizing cells that fixed $^{13}$C-labelled bicarbonate. Red dotted circle: cells that fixed $^{13}$C-bicarbonate without precipitating Fe(III) in the cell vicinity [as consequence of Fe(II) oxidation].
C. Additionally, information on the chemical composition of samples from either of the two approaches can be correlated, which, e.g. allows conclusions on the interaction and distribution of organomineral associations (e.g. ferrous iron/EPS correlation plot). APE, atom per cent enrichment; EPS, extracellular polymeric substances.

biomolecules) with the redox speciation of iron in close proximity to the cell. The mono- or diatomic secondary ions generated by the impact of a high-energy primary ion beam in a NanoSIMS instrument do generally not allow differentiation between the biomolecules from which they originated. However, the fitting of the model spectra of proteins, polysaccharides or lipids to the STXM spectra of a complex environmental sample enables the localization and quantification of major classes of biomacromolecules. Therefore, following a SIP experiment a subsequent analysis of the samples by STXM and NanoSIMS could reveal in which biomolecules the labelled substrate has been incorporated preferentially, similar to what has been shown for single-cell analysis by Raman spectroscopy (Huang *et al*., 2007; Wagner, 2009).

As illustrated by the schematic dataset shown in Fig. 3, the combination of NanoSIMS and STXM holds great promise for mechanistic, process-oriented research in environmental microbiology and biogeochemistry linking data on assimilatory and dissimilatory microbial activities with information on the geochemical microenvironment. The example of microbial chemolithoautotrophic iron oxidation (Fig. 3) is only one conceivable research area that would benefit from the proposed joined application of both techniques. Other potential fields of application are microbially mediated redox reactions, mineral precipitation/dissolution and organic and inorganic contaminant transformation.

Of course combining STXM and NanoSIMS for the chemical imaging of biological samples is technically challenging and will require further method development, mainly with respect to sample preparation and transfer between instruments. In the following section, we will briefly discuss the methodological aspects that need to be considered if both techniques should be applied to the same sample: first of all, STXM should always be performed prior to NanoSIMS, simply because STXM is a relatively non-invasive technique and the sputtering of NanoSIMS will destroy the sample. While for both techniques preservation of the morphological integrity of the sample is important, special precautions are required when it comes to conservation of redox speciation and isotope ratios. For example, in order to prevent oxidation of oxygen-sensitive samples prior to STXM analysis it is essential to prepare and seal samples in an anoxic glove box. Further, for STXM samples need to be soft X-ray transmissible. This requires very thin samples (depending on the chemical composition and density of the sample 40 nm to a few micrometres) that are normally mounted onto 75- to 100-nm-thick silicon nitride ($Si_3N_4$) windows or on polymer-coated TEM grids that might disintegrate under the impact of a high-energy beam during NanoSIMS. This requires that after STXM analysis samples on thin silicon nitride grids need to be lined with a liquid resin that polymerizes underneath the membrane thereby stabilizing the sample mounted on top while keeping its structure and geometry unaltered. This is important because in order to generate overlapping datasets one need to make sure that the same region can be located with high precision within both instruments. This might be achieved by identifying characteristic sample properties or the placement of a landmark on the surface of the sample (e.g. a scratch on the sample support or beam induced marks in close proximity to the sample area of interest) that can be located also with other optical techniques such as light or fluorescence microscopy (Boxer *et al*., 2009). Of course the resin to be used to underlay the sample on the silicon nitride membrane would ideally not interfere with NanoSIMS measurements. Herrmann and colleagues (2007a) evaluated the suitability of various resins for the detection of $^{15}$N-labelled *P. fluorescens* cells in a quartz sand matrix. They found that the $^{14}$N- and $^{15}$N-signals of the epoxy resin Araldite 502 (ProSciTech, Kirwan, Qld, Australia) was uniformly low and did not mask the isotope signal. In these experiments samples were completely embedded. In the case of preparing STXM samples for subsequent analysis by NanoSIMS the resin would just serve as solid sample support only partly in direct contact with the sample through the silicon nitride grid. The $^{12}$C- and $^{14}$N-signals from the resin and the silicon nitride grid, respectively, are not expected to interfere with the carbon or nitrogen isotope signals from SIP experiments of microbial samples.

Irrespective of conquerable methodological challenges with respect to sample treatment one great challenge remains in the end: how can detailed process knowledge on the microscale be integrated into quantitative models that describe, e.g. elemental cycling, transport or the fate of redox-active contaminants at ecosystem scales? This requires that detailed insights into microbial processes and cellular mechanisms gained by high-resolution chemical imaging techniques such as NanoSIMS and STXM be complemented by field observations based on sampling schemes that bridge the scales from the single-cell level to field site dimensions.

## Acknowledgements

We thank E. Swanner, T. Lösekann-Behrens and two anonymous reviewers for their insightful comments and critical reading that improved this manuscript. S. Behrens and A. Kappler were supported by the DFG-funded research training group 'Molecular principles of bacterial survival strategies' (Graduiertenkolleg: GRK1708-1) and DFG grants KA 1736/20-1 and 1736/22-1. M. Obst received support through the Emmy-Noether programme of the DFG (OB 362/1-1).

## References


Behrens, S., Loesekann, T., Pett-Ridge, J., Weber, P.K., Ng, W.-O., Stevenson, B.S., *et al*. (2008) Linking microbial phylogeny to metabolic activity at the single-cell level by using enhanced element labeling-catalyzed reporter deposition fluorescence in situ hybridization (EL-FISH) and NanoSIMS. *Appl Environ Microbiol* **74:** 3143–3150.

Benzerara, K., Menguy, N., Guyot, F., Skouri, F., de Luca, G., Barakat, M., and Heulin, T. (2004a) Biologically controlled precipitation of calcium phosphate by *Ramlibacter tataouinensis*. *Earth Planet Sci Lett* **228:** 439–449.

Benzerara, K., Yoon, T.H., Tyliszczak, T., Constantz, B., Spormann, A.M., and Brown, G.E. (2004b) Scanning transmission X-ray microscopy study of microbial calcification. *Geobiology* **2:** 249–259.

Benzerara, K., Yoon, T.H., Menguy, N., Tyliszczak, T., and Brown, G.E. (2005) Nanoscale environments associated with bioweathering of a Mg-Fe-pyroxene. *PNAS* **102:** 979–982.

Bluhm, H., Andersson, K., Araki, T., Benzerara, K., Brown, G.E., Dynes, J.J., *et al*. (2006) Soft X-ray microscopy and spectroscopy at the molecular environmental science beamline at the Advanced Light Source. *J Electron Spectros Relat Phenomena* **150:** 86–104.

Borch, T., Kretzschmar, R., Kappler, A., Cappellen, P.V., Ginder-Vogel, M., Voegelin, A., and Campbell, K. (2010) Biogeochemical redox processes and their impact on contaminant dynamics. *Environ Sci Technol* **44:** 15–23.

Boxer, S.G., Kraft, M.L., and Weber, P.K. (2009) Advances in imaging secondary ion mass spectrometry for biological samples. *Annu Rev Biophys* **38:** 53–74.

Byrne, M.E., Ball, D.A., Guerquin-Kern, J.-L., Rouiller, I., Wu, T.-D., Downing, K.H., *et al*. (2010) *Desulfovibrio magneticus* RS-1 contains an iron- and phosphorus-rich organelle distinct from its bullet-shaped magnetosomes. *PNAS* **107:** 12263–12268.

Castaing, R., and Slodzian, G. (1962) Microanalyse par émission ionique secondaire (microanalysis by secondary ion emission). *J Microsc* **1:** 395–410.

Chan, C.S., Fakra, S.C., Edwards, D.C., Emerson, D., and Banfield, J.F. (2009) Iron oxyhydroxide mineralization on microbial extracellular polysaccharides. *Geochim Cosmochim Acta* **73:** 3807–3818.

Chan, C.S., Fakra, S.C., Emerson, D., Fleming, E.J., and Edwards, K.J. (2011) Lithotrophic iron-oxidizing bacteria produce organic stalks to control mineral growth: implications for biosignature formation. *ISME J* **5:** 717–727.

Clode, P.L., Kilburn, M.R., Jones, D.L., Stockdale, E.A., Cliff, J.B., III, Herrmann, A.M., and Murphy, D.V. (2009) *In situ* mapping of nutrient uptake in the rhizosphere using nanoscale secondary ion mass spectrometry. *Plant Physiol* **151:** 1751–1757.

Cockell, C.S., van Calsteren, P., Mosselmans, J.F.W., Franchi, I.A., Gilmour, I., Kelly, L., *et al*. (2010) Microbial endolithic colonization and the geochemical environment in young seafloor basalts. *Chem Geol* **279:** 17–30.

Davey, M.E., and O'Toole, G.A. (2000) Microbial biofilms: from ecology to molecular genetics. *Microbiol Mol Biol Rev* **64:** 847–867.

Dekas, A.E., Poretsky, R.S., and Orphan, V.J. (2009) Deep-sea archaea fix and share nitrogen in methane-consuming microbial consortia. *Science* **326:** 422–426.

Deldon, C., Hanselmann, K.W., Peduzzi, R., and Zullig, H. (1985) Phototrophic bacteria in the redox transition zone of Lago Cadagno, a meromictic, alpine lake. *Experientia* **41:** 554–554.

Dohnalkova, A.C., Marshall, M.J., Arey, B.W., Williams, K.H., Buck, E.C., and Fredrickson, J.K. (2011) Imaging hydrated microbial extracellular polymers: comparative analysis by electron microscopy. *Appl Environ Microbiol* **77:** 1254–1262.

Dynes, J.J., Lawrence, J.R., Korber, D.R., Swerhone, G.D.W., Leppard, G.G., and Hitchcock, A.P. (2006a) Quantitative mapping of chlorhexidine in natural river biofilms. *Sci Total Environ* **369:** 369–383.

Dynes, J.J., Tyliszczak, T., Araki, T., Lawrence, J.R., Swerhone, G.D.W., Leppard, G.G., and Hitchcock, A.P. (2006b) Speciation and quantitative mapping of metal species in microbial biofilms using scanning transmission X-ray microscopy. *Environ Sci Technol* **40:** 1556–1565.

Dynes, J.J., Lawrence, J.R., Korber, D.R., Swerhone, G.D.W., Leppard, G.G., and Hitchcock, A.P. (2009) Morphological and biochemical changes in *Pseudomonas fluorescens* biofilms induced by sub-inhibitory exposure to antimicrobial agents. *Can J Microbiol* **55:** 163–178.

Falkowski, P.G., Fenchel, T., and Delong, E.F. (2008) The microbial engines that drive Earth's biogeochemical cycles. *Science* **320:** 1034–1039.

Fayek, M., Utsunomiya, S., Pfiffner, S.M., White, D.C., Riciputi, L.R., Ewing, R.C., *et al*. (2005) The application of HRTEM techniques and nanosims to chemically and isotopically characterize *Geobacter sulfurreducens* surfaces. *Can Mineral* **43:** 1631–1641.

Fike, D.A., Gammon, C.L., Ziebis, W., and Orphan, V.J. (2008) Micron-scale mapping of sulfur cycling across the oxycline of a cyanobacterial mat: a paired nanoSIMS and CARD-FISH approach. *ISME J* **2:** 749–759.

Finzi-Hart, J.A., Pett-Ridge, J., Weber, P.K., Popa, R., Fallon, S.J., Gunderson, T., *et al*. (2009) Fixation and fate of C and N in the cyanobacterium *Trichodesmium* using nanometer-scale secondary ion mass spectrometry. *PNAS* **106:** 6345–6350.

Fischer, C., Wiggli, M., Schanz, F., Hanselmann, K.W., and Bachofen, R. (1996) Light environment and synthesis of bacteriochlorophyll by populations of Chromatium okenii under natural environmental conditions. *FEMS Microbiol Ecol* **21:** 1–9.

Fletcher, J.S., Rabbani, S., Henderson, A., Blenkinsopp, P., Thompson, S.P., Lockyer, N.P., and Vickerman, J.C. (2008) A new dynamic in mass spectral imaging of single biological cells. *Anal Chem* **80:** 9058–9064.

Fletcher, J.S., Lockyer, N.P., and Vickerman, J.C. (2010) Molecular SIMS imaging; spatial resolution and molecular sensitivity: have we reached the end of the road? Is there light at the end of the tunnel? *Surf Interface Anal* **43:** 253–256.

Fletcher, J.S., Lockyer, N.P., and Vickerman, J.C. (2011) Developments in molecular SIMS depth profiling and 3D imaging of biological systems using polyatomic primary ions. *Mass Spectrom Rev* **30:** 142–174.

Foster, R.A., Kuypers, M.M.M., Vagner, T., Paerl, R.W., Musat, N., and Zehr, J.P. (2011) Nitrogen fixation and transfer in open ocean diatom-cyanobacterial symbioses. *ISME J* **5:** 1484–1493.

Frache, G., El Adib, B., Audinot, J.N., and Migeon, H.N. (2011) Evaluation of ionization yields under gallium bombardment. *Surf Interface Anal* **43:** 639–642.

Ghorai, S., and Tivanski, A.V. (2010) Hygroscopic behavior of individual submicrometer particles studied by X-ray spectromicroscopy. *Anal Chem* **82:** 9289–9298.

Gianoncelli, A., Kaulich, B., Alberti, R., Klatka, T., Longoni, A., de Marco, A., *et al*. (2009) Simultaneous soft X-ray transmission and emission microscopy. *Nucl Instrum Methods Phys Res A* **608:** 195–198.

Grovenor, C.R.M., Smart, K.E., Kilburn, M.R., Shore, B., Dilworth, J.R., Martin, B., *et al*. (2006) Specimen preparation for NanoSIMS analysis of biological materials. *Appl Surf Sci* **252:** 6917–6924.

Guerquin-Kern, J.-L., Wu, T.-D., Quintana, C., and Croisy, A. (2005) Progress in analytical imaging of the cell by dynamic secondary ion mass spectrometry (SIMS microscopy). *Biochim Biophys Acta* **1724:** 228–238.

Gutierrez-Zamora, M.-L., and Manefield, M. (2010) An appraisal of methods for linking environmental processes to specific microbial taxa. *Rev Environ Sci Biotechnol* **9:** 153–185.

Halm, H., Musat, N., Lam, P., Langlois, R., Musat, F., Peduzzi, S., *et al*. (2009) Co-occurrence of denitrification and nitrogen fixation in a meromictic lake, Lake Cadagno (Switzerland). *Environ Microbiol* **11:** 1945–1958.

Hanhan, S., Smith, A.M., Obst, M., and Hitchcock, A.P. (2009) Optimization of analysis of soft X-ray spectromicroscopy at the Ca 2p edge. *J Electron Spectros Relat Phenomena* **173:** 44–49.

Heister, K., Höschen, C., Pronk, G.J., Mueller, C.W., and Kögel-Knabner, I. (2011) NanoSIMS as a tool for characterizing soil model compounds and organomineral associations in artificial soils. *J. Soils Sediments* **12:** 35–47.

Henke, B.L., Gullikson, E.M., and Davis, J.C. (1993) X-ray interactions – photoabsorption, scattering, transmission, and reflection at E=50-30,000 eV, Z=1-92. *At Data Nucl Data Tables* **54:** 181–342.

Herrmann, A.M., Clode, P.L., Fletcher, I.R., Nunan, N., Stockdale, E.A., O'Donnell, A.G., and Murphy, D.V. (2007a) A novel method for the study of the biophysical interface in soils using nano-scale secondary ion mass spectrometry. *Rapid Commun Mass Spectrom* **21:** 29–34.

Herrmann, A.M., Ritz, K., Nunan, N., Clode, P.L., Pett-Ridge, J., Kilburn, M.R., *et al*. (2007b) Nano-scale secondary ion mass spectrometry – a new analytical tool in biogeochemistry and soil ecology: a review article. *Soil Biol Biochem* **39:** 1835–1850.

Hitchcock, A.P., Morin, C., Tyliszczak, T., Koprinarov, I.N., Ikeura-Sekiguchi, H., Lawrence, J.R., and Leppard, G.G. (2002) Soft X-ray microscopy of soft matter – hard information from two softs. *Surf Rev Lett* **9:** 193–201.

Hitchcock, A.P., Dynes, J.J., Johansson, G., Wang, J., and Botton, G. (2008a) Comparison of NEXAFS microscopy and TEM-EELS for studies of soft matter. *Micron* **39:** 311–319.

Hitchcock, A.P., Johansson, G.A., Mitchell, G.E., Keefe, M.H., and Tyliszcak, T. (2008b) 3-D chemical imaging using angle-scan nanotomography in a soft X-ray scanning transmission X-ray microscope. *Appl Phys A Mat Sci Process* **92:** 447–452.

Hitchcock, A.P., Dynes, J.J., Lawrence, J.R., Obst, M., Swerhone, G.D.W., Korber, D.R., and Leppard, G.G. (2009) Soft X-ray spectromicroscopy of nickel sorption in a natural river biofilm. *Geobiology* **7:** 432–453.

Hitchcock, A.P., Tylisczcak, T., Obst, M., Swerhone, G.D.W., and Lawrence, J.R. (2010) Improving sensitivity in soft X-ray STXM using low energy X-ray fluorescence. *Microsc Microanal* **16:** 924–925.

Huang, W.E., Stoecker, K., Griffiths, R., Newbold, L., Daims, H., Whiteley, A.S., and Wagner, M. (2007) Raman-FISH: combining stable-isotope Raman spectroscopy and fluorescence *in situ* hybridization for the single cell analysis of identity and function. *Environ Microbiol* **9:** 1878–1889.

Hunter, R.C., Hitchcock, A.P., Dynes, J.J., Obst, M., and Beveridge, T.J. (2008) Mapping the speciation of iron in *Pseudomonas aeruginosa* biofilms using scanning transmission X-ray microscopy. *Environ Sci Technol* **42:** 8766–8772.

Ishihara, M., Ebata, S., Kumondai, K., Mibuka, R., Uchino, K., and Yurimoto, H. (2010) Ultra-high performance multi-turn TOF-SIMS system with a femto-second laser for post-ionization: investigation of the performance in linear mode. *Surf Interface Anal* **42:** 1598–1602.

Johansson, G.A., Tyliszczak, T., Mitchell, G.E., Keefe, M.H., and Hitchcock, A.P. (2007) Three-dimensional chemical mapping by scanning transmission X-ray spectromicroscopy. *J Synchrotron Radiat* **14:** 395–402.

Kaulich, B., Bacescu, D., Cocco, D., Susini, J., Salome, M., Dhez, O., *et al*. (2003) Twinmic: a European twin microscope station combining full-field imaging and scanning microscopy. *J Phys IV* **104:** 103–107.

Kaznatcheev, K.V., Karunakaran, C., Lanke, U.D., Urquhart, S.G., Obst, M., and Hitchcock, A.P. (2007) Soft X-ray spectromicroscopy beamline at the CLS: commissioning results. *Nucl Instrum Methods Phys Res A* **582:** 96–99.

Kilcoyne, A.L.D., Tyliszczak, T., Steele, W.F., Fakra, S., Hitchcock, P., Franck, K., *et al*. (2003) Interferometer-controlled scanning transmission X-ray microscopes at the Advanced Light Source. *J Synchrotron Radiat* **10:** 125–136.

Kirz, J., and Rarback, H. (1985) Soft-X-ray microscopes. *Rev Sci Instrum* **56:** 1–13.

Kirz, J., Jacobsen, C., and Howells, M. (1995) Soft-X-ray microscopes and their biological applications. *Q Rev Biophys* **28:** 33–130.

Lam, K.P., Hitchcock, A.P., Obst, M., Lawrence, J.R., Swerhone, G.D.W., Leppard, G.G., *et al*. (2010) Characterizing magnetism of individual magnetosomes by X-ray magnetic circular dichroism in a scanning transmission X-ray microscope. *Chem Geol* **270:** 110–116.

Lawrence, J.R., Swerhone, G.D.W., Leppard, G.G., Araki, T., Zhang, X., West, M.M., and Hitchcock, A.P. (2003) Scanning transmission X-ray, laser scanning, and transmission electron microscopy mapping of the exopolymeric matrix of microbial biofilms. *Appl Environ Microbiol* **69:** 5543–5554.

Lawrence, J.R., Dynes, J.J., Korber, D.R., Swerhone, G.D.W., Leppard, G.G., and Hitchcock, A.P. (2011) Moni-

toring the fate of copper nanoparticles in river biofilms using scanning transmission X-ray microscopy (STXM). *Chem Geol*. (in press). doi:10.1016/j.chemgeo.2011.07.013.

Lechene, C., Hillion, F., McMahon, G., Benson, D., Kleinfeld, A., Kampf, J.P., *et al*. (2006) High-resolution quantitative imaging of mammalian and bacterial cells using stable isotope mass spectrometry. *J Biol* **5:** 20. doi:10.1186/jbiol42.

Lechene, C.P., Luyten, Y., McMahon, G., and Distel, D.L. (2007) Quantitative imaging of nitrogen fixation by individual bacteria within animal cells. *Science* **317:** 1563–1566.

Li, T., Wu, T.-D., Mazeas, L., Toffin, L., Guerquin-Kern, J.-L., Leblon, G., and Bouchez, T. (2008) Simultaneous analysis of microbial identity and function using NanoSIMS. *Environ Microbiol* **10:** 580–588.

Lin, Y., Trouillon, R., Safina, G., and Ewing, A.G. (2011) Chemical analysis of single cells. *Anal Chem* **83:** 4369–4392.

Metzner, R., Schneider, H.U., Breuer, U., and Schroeder, W.H. (2008) Imaging nutrient distributions in plant tissue using time-of-flight secondary ion mass spectrometry and scanning electron microscopy. *Plant Physiol* **147:** 1774–1787.

Miot, J., Benzerara, K., Morin, G., Kappler, A., Bernard, S., Obst, M., *et al*. (2009a) Iron biomineralization by anaerobic neutrophilic iron-oxidizing bacteria. *Geochim Cosmochim Acta* **73:** 696–711.

Miot, J., Benzerara, K., Obst, M., Kappler, A., Hegler, F., Schadler, S., *et al*. (2009b) Extracellular iron biomineralization by photoautotrophic iron-oxidizing bacteria. *Appl Environ Microbiol* **75:** 5586–5591.

Moore, K.L., Schröder, M., Wu, Z., Martin, B.G.H., Hawes, C.R., McGrath, S.P., *et al*. (2011) High-resolution secondary ion mass spectrometry reveals the contrasting subcellular distribution of arsenic and silicon in rice roots. *Plant Physiol* **156:** 913–924.

Mueller, C.W., Kölbl, A., Hoeschen, C., Hillion, F., Heister, K., Herrmann, A.M., and Kögel-Knabner, I. (2012) Submicron scale imaging of soil organic matter dynamics using NanoSIMS – from single particles to intact aggregates. *Org Geochem* **42:** 1476–1488.

Musat, N., Halm, H., Winterholler, B., Hoppe, P., Peduzzi, S., Hillion, F., *et al*. (2008) A single-cell view on the ecophysiology of anaerobic phototrophic bacteria. *PNAS* **105:** 17861–17866.

Musat, N., Adam, B., and Kuypers, M.M.M. (2011) Nanosecondary ions mass spectrometry (nanoSIMS) coupled with *in situ* hybridization for ecological research. In *Stable Isotope Probing and Related Technologies*. Murrell, J., and Whiteley, A. (eds). Washington, DC, USA: American Society for Microbiology, pp. 295–303.

Neu, T.R., Manz, B., Volke, F., Dynes, J.J., Hitchcock, A.P., and Lawrence, J.R. (2010) Advanced imaging techniques for assessment of structure, composition and function in biofilm systems. *FEMS Microbiol Ecol* **72:** 1–21.

Neufeld, J.D., Wagner, M., and Murrell, J.C. (2007) Who eats what, where and when? Isotope-labelling experiments are coming of age. *ISME J* **1:** 103–110.

Norlund, K.L.I., Southam, G., Tyliszczak, T., Hu, Y., Karunakaran, C., Obst, M., *et al*. (2009) Microbial architecture of environmental sulfur processes: a novel syntrophic sulfur-metabolizing consortia. *Environ Sci Technol* **43:** 8781–8786.

Obst, M., Dynes, J.J., Lawrence, J.R., Swerhone, G.D.W., Benzerara, K., Karunakaran, C., *et al*. (2009a) Precipitation of amorphous $CaCO_3$ (aragonite-like) by cyanobacteria: a STXM study of the influence of EPS on the nucleation process. *Geochim Cosmochim Acta* **73:** 4180–4198.

Obst, M., Wang, J., and Hitchcock, A.P. (2009b) Soft X-ray spectro-tomography study of cyanobacterial biomineral nucleation. *Geobiology* **7:** 577–591.

Orphan, V.J., and House, C.H. (2009) Geobiological investigations using secondary ion mass spectrometry: microanalysis of extant and paleo-microbial processes. *Geobiology* **7:** 360–372.

Orphan, V.J., House, C.H., Hinrichs, K.-U., McKeegan, K.D., and DeLong, E.F. (2001) Methane-consuming archaea revealed by directly coupled isotopic and phylogenetic analysis. *Science* **293:** 484–487.

Orphan, V.J., House, C.H., Hinrichs, K.-U., McKeegan, K.D., and DeLong, E.F. (2002) Multiple archaeal groups mediate methane oxidation in anoxic cold seep sediments. *PNAS* **99:** 7663–7668.

Orphan, V.J., Turk, K.A., Green, A.M., and House, C.H. (2009) Patterns of (15)N assimilation and growth of methanotrophic ANME-2 archaea and sulfate-reducing bacteria within structured syntrophic consortia revealed by FISH-SIMS. *Environ Microbiol* **11:** 1777–1791.

Pantke, C., Obst, M., Benzerara, K., Morin, G., Ona-Nguema, G., Dippon, U., and Kappler, A. (2012) Green rust formation during Fe(II) oxidation by the nitrate-reducing *Acidovorax* sp. strain BoFeN1. *Environ Sci Technol* **46:** 1439–1446.

Ploug, H., Adam, B., Musat, N., Kalvelage, T., Lavik, G., Wolf-Gladrow, D., and Kuypers, M.M.M. (2011) Carbon, nitrogen and O2 fluxes associated with the cyanobacterium *Nodularia spumigena* in the Baltic Sea. *ISME J* **5:** 1549–1558.

Polerecky, L., Adam, B., Milucka, J., Musat, N., Vagner, T., and Kuypers, M.M.M. (2012) Look@NanoSIMS – a tool for the analysis of nanoSIMS data in environmental microbiology. *Environ Microbiol*. (in press). doi:10.1111/j.1462-2920.2011.02681.x.

Popa, R., Weber, P.K., Pett-Ridge, J., Finzi, J.A., Fallon, S.J., Hutcheon, I.D., *et al*. (2007) Carbon and nitrogen fixation and metabolite exchange in and between individual cells of *Anabaena oscillarioides*. *ISME J* **1:** 354–360.

Schanz, F., and Stalder, S. (1998) Phytoplankton summer dynamics and sedimentation in the thermally stratified Lake Cadagno. *Documenta dell'Istituto Italiano di Idrobiologia* **63:** 71–76.

Schanz, F., Fischer-Romero, C., and Bachofen, R. (1998) Photosynthetic production and photoadaptation of phototrophic sulfur bacteria in Lake Cadagno (Switzerland). *Limnol Oceanogr* **43:** 1262–1269.

Templeton, A., and Knowles, E. (2009) Microbial transformations of minerals and metals: recent advances in geomicrobiology derived from synchrotron-based X-ray spectroscopy and X-ray microscopy. In *Annual Review of*

*Earth and Planetary Sciences*. Jeanloz, R., and Freeman, K.H. (eds). Palo Alto, CA, USA: Annual Reviews, pp. 367–391.

Thieme, J., Schneider, G., and Knochel, C. (2003) X-ray tomography of a microhabitat of bacteria and other soil colloids with sub-100 nm resolution. *Micron* **34:** 339–344.

Thieme, J., McNulty, I., Vogt, S., and Paterson, D. (2007) X-ray spectromicroscopy – a tool for environmental sciences. *Environ Sci Technol* **41:** 6885–6889.

Toner, B., Fakra, S., Villalobos, M., Warwick, T., and Sposito, G. (2005) Spatially resolved characterization of biogenic manganese oxide production within a bacterial biofilm. *Appl Environ Microbiol* **71:** 1300–1310.

Tonolla, M., Demarta, A., Peduzzi, R., and Hahn, D. (1999) In situ analysis of phototrophic sulfur bacteria in the chemocline of meromictic Lake Cadagno (Switzerland). *Appl Environ Microbiol* **65:** 1325–1330.

Tonolla, M., Peduzzi, S., Hahn, D., and Peduzzi, R. (2003) Spatio-temporal distribution of phototrophic sulfur bacteria in the chemocline of meromictic Lake Cadagno (Switzerland). *FEMS Microbiol Ecol* **43:** 89–98.

Tonolla, M., Peduzzi, S., Demarta, A., Peduzzi, R., and Hahn, D. (2004) Phototropic sulfur and sulfate-reducing bacteria in the chemocline of meromictic Lake Cadagno, Switzerland. *J Limnol* **63:** 161–170.

Tonolla, M., Peduzzi, R., and Hahn, D. (2005) Long-term population dynamics of phototrophic sulfur bacteria in the chemocline of Lake Cadagno, Switzerland. *Appl Environ Microbiol* **71:** 3544–3550.

Tourna, M., Stieglmeier, M., Spang, A., Könneke, M., Schintlmeister, A., Urich, T., *et al*. (2011) *Nitrososphaera viennensis*, an ammonia oxidizing archaeon from soil. *PNAS* **108:** 8420–8425.

Wagner, M. (2009) Single-cell ecophysiology of microbes as revealed by raman microspectroscopy or secondary ion mass spectrometry imaging. *Annu Rev Microbiol* **63:** 411–429.

Wang, J., Zhou, J., Fang, H., Sham, T.-K., Karunakaran, C., Lu, Y., *et al*. (2011) Effect of humidity on individual SnO(2) coated carbon nanotubes studied by in situ STXM. *J Electron Spectros Relat Phenomena* **184:** 296–300.

Warwick, T., Franck, K., Kortright, J.B., Meigs, G., Moronne, M., Myneni, S., *et al*. (1998) A scanning transmission x-ray microscope for materials science spectromicroscopy at the advanced light source. *Rev Sci Instrum* **69:** 2964–2973.

Watrous, J.D., and Dorrestein, P.C. (2011) Imaging mass spectrometry in microbiology. *Nat Rev Microbiol* **9:** 683–694.

Webb, H.K., Truong, V.K., Hasan, J., Crawford, R.J., and Ivanova, E.P. (2011) Physico-mechanical characterisation of cells using atomic force microscopy – current research and methodologies. *J Microbiol Methods* **86:** 131–139.

Willingham, D., Kucher, A., and Winograd, N. (2008) Molecular depth profiling and imaging using cluster ion beams with femtosecond laser postionization. *Appl Surf Sci* **255:** 831–833.

Winograd, N., and Garrison, B.J. (2010) Biological cluster mass spectrometry. *Annu Rev Phys Chem* **61:** 305–322.